UCLA
UCLA Previously Published Works

Title

Single-molecule FRET reveals sugar-induced conformational dynamics in LacY

Permalink

https://escholarship.org/uc/item/5r94t3wg

Journal

Proceedings of the National Academy of Sciences of the United States of America, 104

ISSN

0027-8424

Authors

Nir, Eyal
Kong, Xiangxu
Weiss, Shimon
et al.

Publication Date

2007-07-01

Peer reviewed

Single-molecule FRET Reveals a Sugar-Induced Conformational Dynamics in LacY

Devdoot S. Majumdar[1], Irina Smirnova[2], Vladimir Kasho[2], Eyal Nir[3], Xiangxu Kong[3], Shimon Weiss[1,2,3,5,*] and H. Ronald Kaback[1,2,4,*]

[1]Molecular Biology Institute, [2]Departments of Physiology, [3]Department of Chemistry and Biochemistry, [4]Department of Microbiology, Immunology & Molecular Genetics, [5]California NanoScience Institute, University of California Los Angeles, CA 90095-1662

*To whom correspondence should be addressed: H.R.K.-- (kaback@mednet.ucla.edu); Tel.: (310) 206-5053. Fax: (310) 206-8623; S.W.-- (sweiss@chem.ucla.edu); Tel: (310) 267-4641, Fax: (310) 267-4672

Abbreviations. A, acceptor; ALEX, alternating laser exciation; D, donor; DDM, dodecyl-ß-D-maltopyranoside; FRET, Fluorescence (Förster) resonance energy transfer; sm-FRET, single-molecule fluorescence resonance energy transfer; NPG, 4-nitrophenyl-α-D-galactopyranoside ; NPGlc, 4-nitrophenyl-α-D-glucopyranoside; E^*, apparent FRET efficiency; $<E^*>$, average E^*; ΔE^*, width of E^* distribution; E, FRET efficiency; $<E>$, average FRET efficiency; S, stoichiometry ratio; R_0, Förster radius.

The N- and C-terminal 6-helix bundles of lactose permease (LacY) form a large internal cavity open on the cytoplasmic side and closed on the periplasmic side with a single sugar-binding site at the apex of the cavity near the middle of the molecule. During sugar/H$^+$ symport, an outward-facing cavity is thought to open with closing of the inward-facing cavity so that the sugar-binding site is alternately accessible to either face of the membrane. In this communication, single molecule Fluorescence (Förster) Resonance Energy Transfer (sm-FRET) is used to test this model with wild-type LacY and a conformationally restricted mutant. Pairs of Cys residues at the ends of two helices on the cytoplasmic or periplasmic sides of wild-type LacY and the mutant were labeled with appropriate donor and acceptor fluorophores, sm-FRET was determined in the absence and presence of sugar and distance changes were calculated. With wild-type LacY, binding of a galactopyranoside, but not a glucopyranoside, results in a decrease in distance on the cytoplasmic side and an increase in distance and in distance distribution on the periplasmic side. In contrast, with the mutant, a more pronounced decrease in distance and in distance distribution is observed on the cytoplasmic side, but there is no change on the periplasmic side. The results are consistent with the alternating access model and indicate that the translocation defect in the mutant is due to ineffective occupancy of the outward-facing conformation.

The lactose permease of *Escherichia coli* (LacY), a member of the Major Facilitator Superfamily, utilizes free energy stored in an electrochemical H^+ gradient ($\triangle\mu_{H+}$) to drive active transport by coupling the downhill, stoichiometric translocation of H^+ with $\triangle\mu_{H+}$ to the uphill accumulation of galactopyranosides. Conversely, in the absence of $\Delta\mu_{H+}$, LacY utilizes free energy released from downhill translocation of galactosides in either direction to drive uphill translocation of H^+ with generation of $\Delta\mu_{H+}$ {reviewed in (1)}.

An X-ray structure of mutant C154G, which binds ligand as well as wild-type LacY but catalyzes very little transport and is compromised conformationally (2-5), has been solved in an inward-facing conformation with bound ligand (6, 7). Notably, wild-type LacY has the same global fold (1, 8). The symporter contains 12 transmembrane α-helices organized in two pseudo-symmetrical bundles. The N- and C-terminal 6-helix bundles form a large internal cavity open to the cytoplasm, and a single sugar-binding site is present at the apex of the cavity near the approximate middle of the molecule.

When compared to the X-ray structure, distances approximated from cross-linking of paired Cys residues across the inward-facing cavity are underestimated, and there is no access to the sugar-binding site from the external surface (6). Therefore, it was suggested that during transport the inward-facing cavity closes with opening of an outward-facing cavity so that the sugar-binding site is alternately accessible to either face of the membrane, and a similar model was proposed for the glycerol phosphate/phosphate antiporter

GlpT (9), a related protein. Recent findings (10) from site-directed alkylation of Cys residues at almost every position in LacY support the alternating access model.

The heat of ligand binding to wild-type LacY and the C154G mutant has been measured (11). The affinity of wild-type or mutant LacY for ligand and the change in free energy (ΔG) upon binding are similar. However, in the wild type, ΔG is due primarily to an increase in entropy, while in marked contrast, an increase in enthalpy is responsible for ΔG in the mutant. Thus, wild-type LacY behaves as if there are multiple ligand-bound conformational states, while the mutant is severely restricted.

sm-FRET (12-14) has been applied to the study of relatively few membrane proteins (eg. F_1F_o-ATP synthase (15), epidermal growth factor (16), and SNARE proteins (17, 18)). Structural dynamics in these proteins has been probed by measuring sm-FRET either from freely diffusing molecules or by recording a time-trajectory from a single, immobilized protein.

Here we utilize sm-FRET by alternating laser excitation (ALEX) spectroscopy (19-22) to study ligand-induced distance changes on the cytoplasmic and periplasmic sides of the membrane protein LacY, freely diffusing in detergent micelles. The results provide further support for the alternating access model in wild-type LacY and suggest that although the cytoplasmic cavity also closes in the C154G mutant, the periplasmic side remains closed in the presence of ligand. The results are also support the conclusion (11) that sugar

binding induces primarily an entropic change in wild-type LacY, in marked contrast to mutant C154G, which exhibits an enthalpic change.

Results

Mutants. Cysteine pairs were introduced into wild type and C154G LacY. None of the native Cys residues in LacY react with maleimides under near stoichiometric conditions except for Cys148, which is readily protected by substrate (23). Two mutant pairs – R73C/S401C (helices III and XII) on the cytoplasmic side and I164C/S375C (helices V and XI) on the periplasmic side – satisfy the following requirements: (i) both positions are at the ends of transmembrane helices; (ii) individual Cys replacements have little or no effect on lactose transport (24-27): (iii) Cys residues at each of the four positions react with the maleimide-based Alexa dyes (Table 1); (iv) double-Cys mutants labeled with fluorophores bind sugar effectively (Table 1); and (v) distances between bound fluorophores in both double-Cys mutants are within R_o for the Alexa dyes used (~50 Å).

Since the size of both Alexa moieties is significant, the inter-dye distance depends on the relative orientation of the dyes as determined by the mobility of the fluorophores and the structural flexibility of LacY. Structural modeling (see *Supporting Information*) predicts different orientations of the donor (D)-acceptor (A) pairs on either side of the protein; these positions are likely to be relatively rigid due to placement in α-helices (Figure 1). Approximate distances between D and A moieties are 48 Å for the cytoplasmic pair or 61 Å for periplasmic pair,

distances that fall well within the linear range of the sm-FRET "ruler," as they are near R_0 of both Alexa dyes (see *Materials & Methods*).

Each of the four double-labeled samples displays significant FRET. However, mutants labeled with D-only or A-only and then mixed exhibit no FRET whatsoever. Thus, there is little or no aggregation. It is also notable that changes in FRET are not observed in the presence of galactopyranosides when ensemble measurements are carried out with a conventional fluorimeter (data not shown).

Structural Changes at the Cytoplasmic Side. sm-FRET is determined from bursts of fluorescence detected during diffusion of labeled molecules through a focused laser beam using ALEX spectroscopy (20). Bursts are recognized by a dual-channel burst search, which identifies bursts containing both D and A (28). For each burst, the apparent energy transfer efficiency (or proximity ratio, E^*), and the stoichiometry (S) are calculated and binned into a two-dimensional (2D) S-E^* histogram (Figure 2A and 4A). D-only and A-only populations are filtered out and E^* values of the D-A species are projected onto a one dimensional (1D) FRET histogram (Figures 2B, 2C, 3A, 4B, 4C).

Each sample was monitored for changes in E^* in response to a relatively high-affinity ligand, 4-nitrophenyl-α-D-*galacto*pyranoside (NPG), or the analogue, 4-nitrophenyl-α-D-*gluco*pyranoside (NPGlc), which exhibits no detectable binding (29-31). R73C/S401C LacY double-labeled on the cytoplasmic side (helices III and XII) exhibits a E^* distribution with mean $<E^*> = 0.536 \pm 0.013$ (Figures 2A, panel 1 and 2B, grey area). Addition of NPG results in small but reproducible

shift to $<E^*> = 0.584 \pm 0.009$ (Figure 2B, red line), consistent with a small but reproducible decrease in distance. No effect of NPGlc ($<E^*> = 0.547 \pm 0.001$) is observed (Figure 2B, blue line). In contrast, mutant C154G, which is conformationally restricted (4, 5, 11) and labeled at the same positions, exhibits $<E^*> = 0.512 \pm 0.007$ (Figures 2A, panel 4 and 2C, grey area), suggesting a slight increase in distance relative to the wild-type (compare Figure 2B and 2C, grey areas). More dramatically, addition of NPG results in a significant shift, $<E^*> = 0.611 \pm 0.007$, indicating a reduction in distance between D and A (Figure 2C, red line). Since addition of NPGlc has no effect whatsoever (Figure 2C, blue line), it is concluded that the changes in the E^* distribution are specific to the galactopyranoside ring.

To test further the binding specificity of NPG to the double-labeled R73C/S401C/C154G LacY mutant, E^* histograms were recorded as a function of NPG concentration (Figure 3A). The relative changes (see definition in *Supporting Information)* in the average E ($<E>$) and in the average width of the distribution ($<\Delta E^*>$) are plotted as a function of NPG concentration in Figure 3B. Increasing NPG concentration is accompanied by a shift in $<E^*>$ to higher values with a concomitant decrease in $<\Delta E^*>$. Apparent K_D values extracted from the $<E^*>$ and $<\Delta E^*>$ titration curves are 40 ± 14 μM and 52 ± 14 μM respectively. These values are in good agreement with those obtained by using other methods (4, 31).

Each cysteine position described herein was labeled individually with D and A on both wild type and C154G backgrounds. The quantum yield of D-

labeled molecules and spectral overlap of D and A was used to calculate R_0 for each construct. Furthermore, because conversion from E* to E relies on an approximation to obtain the γ-correction factor (see *Supplementary Materials*), we achieve approximate E values and corresponding inter-dye distances. On the cytoplasmic side, the average distances between dyes are calculated to be ~51.3 Å for wild type and ~53.3 Å for C154G LacY without bound sugar (Table 2), which are in general agreement with modeling (Figure 1). NPG binding to wild type LacY is associated with a small decrease in distance (~1.6 Å), while the C154G mutant exhibits a larger decrease of ~3.6 Å and a narrowing of <ΔE*> (Fig. 3).

Structural Changes at the Periplasmic Side. Analysis of E* distribution for I164C/R375C LacY double-labeled on the periplasmic side (helices V and XI) exhibits <E*> = 0.416 ± 0.004 (Figures 4A, panel 1 & 4B, grey area). Addition of NPG results in a shift to <E*> = 0.344 ± 0.004, indicating an increase in the distance between the dyes upon ligand binding (Figure 4B, red line). NPGlc addition results in no significant change in the E* distribution (Figure 4B, blue line). C154G LacY labeled at the same positions exhibits <E*> = 0.360 ± 0.001, and addition of neither NPG nor NPGlc produces a significant change (Figure 4C).

The average distances between dyes are calculated to be ~56.9 Å for wild type and ~57.8 Å for C154G LacY without bound sugar (Table 2) based on determined R_0. NPG binding to wild type is associated with an increase in

distance (~3.5 Å) and a slight increase in $<\Delta E^*>$, while the C154G mutant exhibits no significant change.

Discussion

sm-FRET is utilized here to investigate the effects of sugar binding on local distance and distance distribution changes between the cytoplasmic ends of helices III and XII or the periplasmic ends of helices V and XI in wild-type LacY and the conformationally restricted mutant C154G. The measured inter-dye distances calculated from sm-FRET are comparable to those predicted from modeling (compare Figure 1 with Table 2). While sugar binding in the wild type background appears to decrease distance (i.e., increased $<E^*>$) between the cytoplasmic ends of helices III and XII, the effect is significantly more pronounced in the mutant background and is also accompanied by a reduction in $<\Delta E^*>$. In marked contrast, the periplasmic ends of helices V and XI appear to move apart (i.e., decreased $<E^*>$) as a result of sugar binding in the wild type, but no change whatsoever is detected with the C154G mutant (Table 2).

Analysis of the shape of the E^* histogram provides information about static distance changes, as well as changes in the distribution of conformers and interconversion rates between them (28). The shape of the E^* histogram of a single conformer (a single E^* value) is determined by shot noise. Multiple conformers (multiple E^* values) result in broadening or splitting of the E^* histogram. If each conformer is long-lived (longer than the transit time through the confocal volume), the resulting histogram will be a superposition of the

individual shot-noise broadened states. If the interconversion between conformers is faster than the transit time, the E* distribution averages out to a single E* value (broadened by shot noise). When interconversion between conformers is on the order of the transit time, the resulting histogram width is dependent on the rates.

Both wild-type and C154G LacY without and with ligand, exhibit conformational heterogeneity on the cytoplasmic and periplasmic sides (distributions are wide and not limited by shot noise; see Fig. S1). The distance and distance distribution changes may be due to interconversion between two states (minimally) at rates that are about 10 times slower than diffusion (interconversion rates faster than diffusion would result in narrower peaks; slower rates do not fit the data--see Figure S2). An alternative possibility is that the wild type and the mutant have multiple static conformers in the unliganded state, and upon binding, the number of conformers is reduced for the mutant and increased for the wild type. For detailed discussion, see *Supplemental Information*.

The sm-FRET findings with wild-type LacY are consistent with extensive site-directed alkylation studies (10) that support an alternating access model for galactoside/H$^+$ symport (1, 6). By this means, the single sugar-binding site in LacY in the approximate middle of the molecule is alternately exposed to either side of the membrane due to opening and closing of cytoplasmic and periplasmic hydrophilic cavities. In this regard, it is particularly noteworthy that the cytoplasmic ends of helices III and XII in the C154G mutant apparently move closer upon sugar binding, while the periplasmic ends of helices V and XI exhibit

no change. The observations suggest that the C154G mutation may markedly decrease the ability of LacY to occupy an outward-facing conformation, thereby drastically inhibiting all modes of sugar translocation (4, 5).

The crystal structure of wild-type LacY exhibits an inward-facing conformation much like the C154G mutant (1, 8). Furthermore, ligand binding markedly increases the apparent accessibility/reactivity of a number of engineered Cys residues on the periplasmic side of the sugar-binding site with a distribution suggesting that sugar binding opens a hydrophilic pathway on the periplasmic side of the molecule. Thus, it seems reasonable to conclude that the crystal structure of LacY is similar to that in the membrane--the inward-facing conformation. If this is so, the time of occupancy in the outward-facing conformation is likely to be relatively short since the inward-facing conformation probably represents the lowest free-energy state.

Taken together, isothermal scanning calorimetry studies (11), site-directed alkylation studies (10) and the sm-FRET studies presented here (carried out on only two pairs of helices thus far) are consistent with a picture in which ligand binding leads primarily to an entropic change in the wild type and an enthalpic change in the C154G mutant. Thus, wild-type LacY behaves as if there are multiple ligand-bound conformational states, while the mutant is severely restricted due to an inability to occupy the outward-facing conformation. Moreover, the findings are consistent with the notion that cytoplasmic and periplasmic movements of the helices in LacY are not necessarily coordinated, a consideration that may be related to the irregular nature of many of the helices.

It follows that the N- and C-terminal helical bundles in LacY probably do not move as rigid bodies.

Figure 5 proposes a simple cartoon model for the conclusions.

Materials and Methods

Fluorophores. Alexa 488 C_5-maleimide and Alexa 647 C_2-maleimide fluorophores were purchased from Molecular Probes (Invitrogen, Carlsbad, CA).

Labeling of LacY mutants with Alexa dyes. Mutants with single additional Cys residue (40-50 μM) were incubated with equimolar concentrations of either Alexa Fluor 488 C_5-maleimide, or Alexa Fluor 647 C_2-maleimide in 50 mM NaP$_i$ buffer, pH 7.0, 0.02% DDM in the presence of 15 mM TDG added for protection of Cys148 against alkylation. The reaction was carried out for 30 min at room temperature in the dark. Double-Cys mutants were labeled in the same buffer sequentially, first with equimolar concentration of Alexa Fluor 647 C_2-maleimide for 30 min in the dark, then Alexa Fluor 488 C_5-maleimide was added and reaction was carried out for another 45 min. TDG and unreacted fluorophores were removed by buffer exchange on Amicon Ultra-15 concentrator with cut-off MW 30 kDa (Millipore, Bedford, MA). The extent of the labeling was estimated from absorption spectra of labeled mutants by measuring peak maxima at 280, 488 and 647 nm for protein and fluorophores, respectively using Hitachi model 24 UV-VIS scanning spectrophotometer (Hitachi, Japan). Control experiments with labeling under the same conditions of either WT or C154G/LacY that lack introduced Cys pairs resulted in no significant incorporation of Alexa dyes. Final samples (0.5 mg/ml) were frozen in liquid nitrogen and stored at -80°C before use.

Binding Assays. Sugar binding to purified LacY mutants was measured before and after labeling with Alexa fluorophores using direct sugar binding assay based on Trp151-NPG FRET as described recently (31). Trp emission spectra (excitation 295 nm) of LacY mutants (0.4 μM) in 50 mM NaP$_i$ (pH 7.5)/0.02% DDM were recorded first in the presence of 100 μM of NPG, then after addition of 10 mM of TDG used for displacement of bound NPG. Relative Trp fluorescence increase after TDG addition quantified the level of specific sugar binding. Spectral properties of used Alexa fluorophores do not interfere with Trp-NPG FRET. The ability of LacY mutants modified with Alexa fluorophores to bind NPG was 70-100% of that for LacY before modification.

Sample Preparation. For measurement, LacY was diluted to 200 pM in 50 mM sodium phosphate, pH 7.5/0.02% DDM, 100 μg/ml bovine serum albumin with or without sugar. An observation chamber for a 5 μl drop was constructed using an 8 mm hole in a 0.5-mm-thick silicone gasket between two No. 1 coverslips.

Microscope Setup, Data Collection and Analysis. Measurements were made using an oil-immersion objective (Zeiss 100X1.4 NA) inverted fluorescence microscope, described elsewhere. Molecules were excited by ALEX (20) at 470 nm and 640 nm (Toptica Photonics iPulse and iBeam, respectively) with an alternation period of 100 μs and a duty cycle of 50%. Excitation intensities were 50-60 μW for 470 nm and 10 μW for 640 nm. The beam was focused by an oil-immersion objective. Fluorescence was collected through the same objective and refocused onto a 100 μm pinhole to reject out-of-focus light. The collected

photons were split by a dichroic mirror (630DRLP, OMEGA Optical, Brattleboro, VT), filtered (540-DF-40; Donor, 660-LP Acceptor) and detected by avalanche photodiodes (SPCM-AQR-14, PerkinElmer, Fremont, CA). Time of arrival of each detected photon was stored on a computer for future analysis (28). Data was typically collected for 10-15 min, yielding ~3000 bursts. Each experiment was repeated 3 – 5 times. Results (and their errors) were calculated from these data sets. A detailed descriptions of data analysis and fitting protocols are given in *Supporting Information*.

All other materials, construction of mutants, purification of proteins, ensemble fluorescence measurements, molecular modeling and smFRET data analysis are described in *Supporting Information.*

References

1. Guan, L. & Kaback, H. R. (2006) *Annu Rev Biophys Biomol Struct* **35,** 67-91.

2. Menick, D. R., Sarkar, H. K., Poonian, M. S., & Kaback, H. R. (1985) *Biochem Biophys Res Commun* **132,** 162-170.

3. van Iwaarden, P. R., Driessen, A. J., Lolkema, J. S., Kaback, H. R., & Konings, W. N. (1993) *Biochemistry* **32,** 5419-5424.

4. Smirnova, I. N. & Kaback, H. R. (2003) *Biochemistry* **42,** 3025-3031.

5. Ermolova, N. V., Smirnova, I. N., Kasho, V. N., & Kaback, H. R. (2005) *Biochemistry* **44,** 7669-7677.

6. Abramson, J., Smirnova, I., Kasho, V., Verner, G., Kaback, H. R., & Iwata, S. (2003) *Science* **301,** 610-615.

7. Mirza, O., Guan, L., Verner, G., Iwata, S., & Kaback, H. R. (2006) *Embo J* **25,** 1177-1183.

8. Guan, L., Smirnova, I. N., Verner, G., Nagamoni, S., & Kaback, H. R. (2006) *Proc Natl Acad Sci U S A* **103,** 1723-1726.

9. Huang, Y., Lemieux, M. J., Song, J., Auer, M., & Wang, D. N. (2003) *Science* **301,** 616-620.

10. Kaback, H. R., Dunten, R., Frillingos, S., Venkatesan, P., Kwaw, I., Zhang, W., & Ermolova, N. (2006) *Proc Natl Acad Sci U S A*.

11. Nie, Y., Smirnova, I., Kasho, V., & Kaback, H. R. (2006) **281,** 35779-35784.

12.   Deniz, A. A., Laurence, T. A., Beligere, G. S., Dahan, M., Martin, A. B., Chemla, D. S., Dawson, P. E., Schultz, P. G., & Weiss, S. (2000) *Proceedings of the National Academy of Sciences of the United States of America* **97,** 5179-5184.

13.   Ha, T., Enderle, T., Ogletree, D. F., Chemla, D. S., Selvin, P. R., & Weiss, S. (1996) *Proceedings of the National Academy of Sciences of the United States of America* **93,** 6264-6268.

14.   Weiss, S. (1999) *Science* **283,** 1676-1683.

15.   Diez, M., Zimmermann, B., Borsch, M., Konig, M., Schweinberger, E., Steigmiller, S., Reuter, R., Felekyan, S., Kudryavtsev, V., Seidel, C. A.*, et al.* (2004) *Nature structural & molecular biology* **11,** 135-141.

16.   Sako, Y., Minoghchi, S., & Yanagida, T. (2000) *Nature cell biology* **2,** 168-172.

17.   Margittai, M., Widengren, J., Schweinberger, E., Schroder, G. F., Felekyan, S., Haustein, E., Konig, M., Fasshauer, D., Grubmuller, H., Jahn, R.*, et al.* (2003) *Proceedings of the National Academy of Sciences of the United States of America* **100,** 15516-15521.

18.   Weninger, K., Bowen, M. E., Chu, S., & Brunger, A. T. (2003) *Proceedings of the National Academy of Sciences of the United States of America* **100,** 14800-14805.

19.   Kapanidis, A. N., Laurence, T. A., Lee, N. K., Margeat, E., Kong, X., & Weiss, S. (2005) *Accounts of chemical research* **38,** 523-533.

20. Kapanidis, A. N., Lee, N. K., Laurence, T. A., Doose, S., Margeat, E., & Weiss, S. (2004) *Proc Natl Acad Sci U S A* **101,** 8936-8941.

21. Kapanidis, A. N., Margeat, E., Ho, S. O., Kortkhonjia, E., Weiss, S., & Ebright, R. H. (2006) *Science* **314,** 1144-1147.

22. Lee, N. K., Kapanidis, A. N., Wang, Y., Michalet, X., Mukhopadhyay, J., Ebright, R. H., & Weiss, S. (2005) *Biophys J* **88,** 2939-2953.

23. le Coutre, J., Whitelegge, J. P., Gross, A., Turk, E., Wright, E. M., Kaback, H. R., & Faull, K. F. (2000) *Biochemistry* **39,** 4237-4242.

24. Sahin-Tóth, M., Frillingos, S., Bibi, E., Gonzalez, A., & Kaback, H. R. (1994) *Protein Sci* **3,** 2302-2310.

25. Frillingos, S. & Kaback, H. R. (1996) *Biochemistry* **35,** 5333-5338.

26. He, M. M., Sun, J., & Kaback, H. R. (1996) *Biochemistry* **35,** 12909-12914.

27. Frillingos, S., Sahin-Toth, M., Wu, J., & Kaback, H. R. (1998) *Faseb J* **12,** 1281-1299.

28. Nir, E., Michalet, X., Hamadani, K. M., Laurence, T. A., Neuhauser, D., Kovchegov, Y., & Weiss, S. (2006) *J Phys Chem B Condens Matter Mater Surf Interfaces Biophys* **110,** 22103-22124.

29. Rudnick, G., Schuldiner, S., & Kaback, H. R. (1976) *Biochemistry* **15,** 5126-5131.

30. Sahin-Tóth, M., Gunawan, P., Lawrence, M. C., Toyokuni, T., & Kaback, H. R. (2002) *Biochemistry* **41,** 13039-13045.

31. Smirnova, I. N., Kasho, V. N., & Kaback, H. R. (2006) *Biochemistry* **45,** 15279-15287.

32. Nir, E., Michalet, X., Hamadani, K. M., Laurence, T. A., Neuhauser, D., Kovchegov, Y., & Weiss, S. (2006) *J Phys Chem B Condens Matter Mater Surf Interfaces Biophys* **110,** 22103-22124.

Tables

Table 1: Properties of cysteine LacY mutants double labeled by Alexa488 and Alexa647 fluorophores.

LacY mutant	Extent of labeling[a] (mol per mol of protein)		NPG binding[b] (% of binding to non-labeled mutant)
	A488	A647	
R73C/S401C/WT	0.6	0.6	98
R73C/S401C/C154G	0.7	0.8	93
I164C/S375C/WT	1	0.7	79
I164C/S375C/C154G	0.8	0.8	93

[a] estimated from absorption spectra (see *Material and Methods*)

[b] detected by direct sugar binding assay based on Trp-NPG FRET as described in Material and Methods (31)

Table 2:   Effect of sugar binding on sm-FRET parameters

Location of double-labeled Cys pairs		No sugar			NPG (1 (15))			NPGlc (1 (15))			NPG induced distance change, Å
		E*	E[a]	Dist. (Å)[b]	E*	E	Dist (Å)	E*	E	Dist (Å)	
Cytoplasmic side	WT	0.536 (±0.013)	0.468 (±0.013)	51.5	0.584 (±0.009)	0.523 (±0.009)	49.7	0.547 (±0.001)	0.480 (±0.001)	51.1	1.4 - 1.8 decrease
73/401	154G	0.512 (±0.007)	0.444 (±0.008)	53.1	0.611 (±0.007)	0.552 (±0.009)	49.5	0.523 (±0.026)	0.456 (±0.030)	52.7	3.5 - 3.7 decrease
Periplasmic side	WT	0.416 (±0.004)	0.342 (±0.003)	56.8	0.344 (±0.004)	0.264 (±0.004)	60.4	0.411 (±0.010)	0.336 (±0.011)	57.0	3.4 - 3.6 increase
164/375	154G	0.360 (±0.001)	0.282 (±0.001)	57.8	0.363 (±0.010)	0.283 (±0.008)	57.8	0.359 (±0.001)	0.279 (±0.002)	57.9	No significant change

[a] E is a corrected sm-FRET efficiency (22)

[b] Distances have precision of ±1 Å.

Figure Legends

Figure 1. Structural modeling of LacY double-labeled with Alexa fluorophores at Cys-pairs introduced at the cytoplasmic ends of helices III and XII (R73C/S401C) (left) or the periplasmic ends of helices V and XI (I164C/R375C) (right). Backbone of LacY rendered as ribbons rainbow colored from blue (helix 1) to red (helix 12) with hydrophilic cavity open to cytoplasmic side. Attached fluorophores colored in green (Alexa488) or magenta (Alexa647) and shown in space filling representation. Estimated distances between C_α atoms of the Cys pairs and between centers of the fluorophores are 41 and 48 Å (cytoplasmic), and 32 and 61 Å (periplasmic), respectively.

Figure 2. Ligand-induced effects on the FRET distribution E* at the cytoplasmic side of LacY (R73C/S401C, helices III and XII). *(A)* 2D S-E* histograms corresponding to wild-type (*A1-A3*) and C154G mutant (*A4-A6*) LacY. Measurements for each construct were obtained in the absence of sugar (*A1, A3)* and in the presence of 1 mM (saturating) NPG concentration (*A2, A4*), or 1 mM NPGlc (*A3, A6*). Comparison of sugar effects on normalized E* histograms from panel A for: *(B)* wild type LacY and for *(C)* C154G LacY. Gray bins, no sugar added; red line, 1 mM NPG; blue line, 1 mM NPGlc. Broken lines, Gaussian fits to the data with the corrected E values given in Table 2.

Figure 3. Concentration dependence of ligand-induced effects on <E*> and ΔE* at the cytoplasmic side of LacY (R73C/S401C/C154G, helices III and XII). *(A)* E* distribution without added sugar (red) and with nine NPG concentrations increasing from 1 µM (orange) to 1000 µM (purple). *(B)* Fractional change of the fitted Gaussian parameters of histograms from panel A plotted as a function of NPG concentration. Red, relative <E*> shift; black, relative ΔE* change. Solid lines, hyperbolic fit to each data set; broken line, theoretical curve showing NPG binding to LacY with K_D of 38 μM as measured by stopped-flow (31).

Figure 4. Ligand-induced effects on the FRET distribution E* at the periplasmic side of LacY (I164C/S375C, helices V and XI). All details are as described in Figure 2.

Figure 5. Cartoon model illustrating global conformational changes detected by smFRET upon sugar binding to wild type LacY (A) and C154G mutant (B). Without bound sugar (left) protein is in protonated state with inward-facing hydrophilic cavity. This conformation is the most energetically stable among multiple unliganded conformers. Binding of sugar induces a global conformational change in both wild type LacY (A, right) and C154G mutant (B, right) resulting in closing of inward-facing hydrophilic cavity. The periplasmic cavity opens in wild type LacY (A, right) allowing substrate to be released . Conformational heterogeneity of wild type LacY increases after sugar binding. In contrast, the periplasmic cavity in C154G mutant does not form easily after sugar

binding (B, right), corresponding to reduced number of conformers in ligand bound state and restricted access for the sugar from periplasmic side.
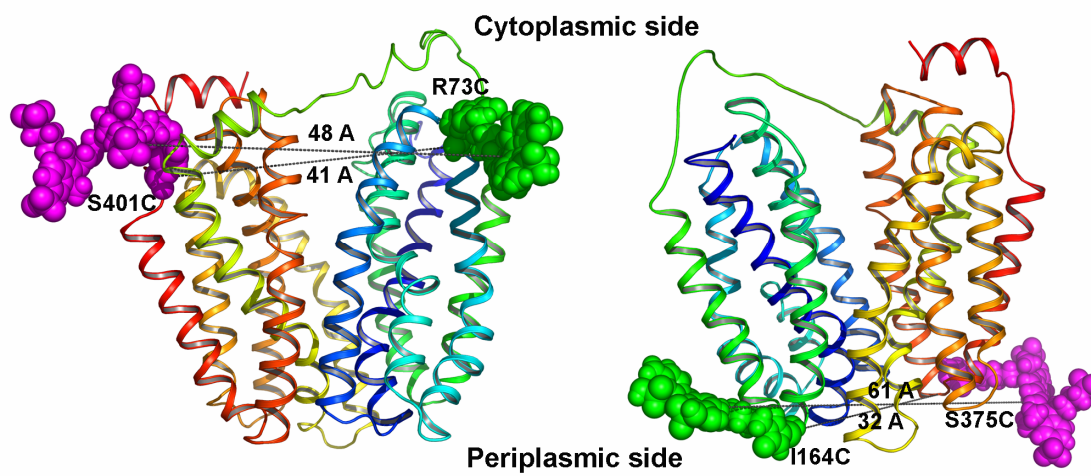
Cytoplasmic side

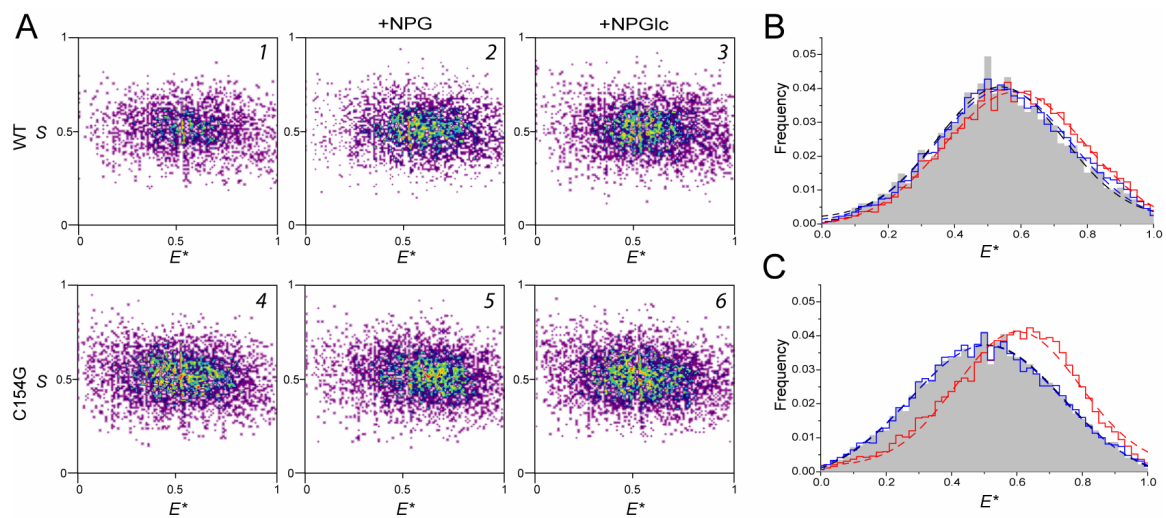R73C

S401C

48 A

41 A

Periplasmic side

61 A

32 A

I164C

S375C

Figure 1   Majumdar et al.

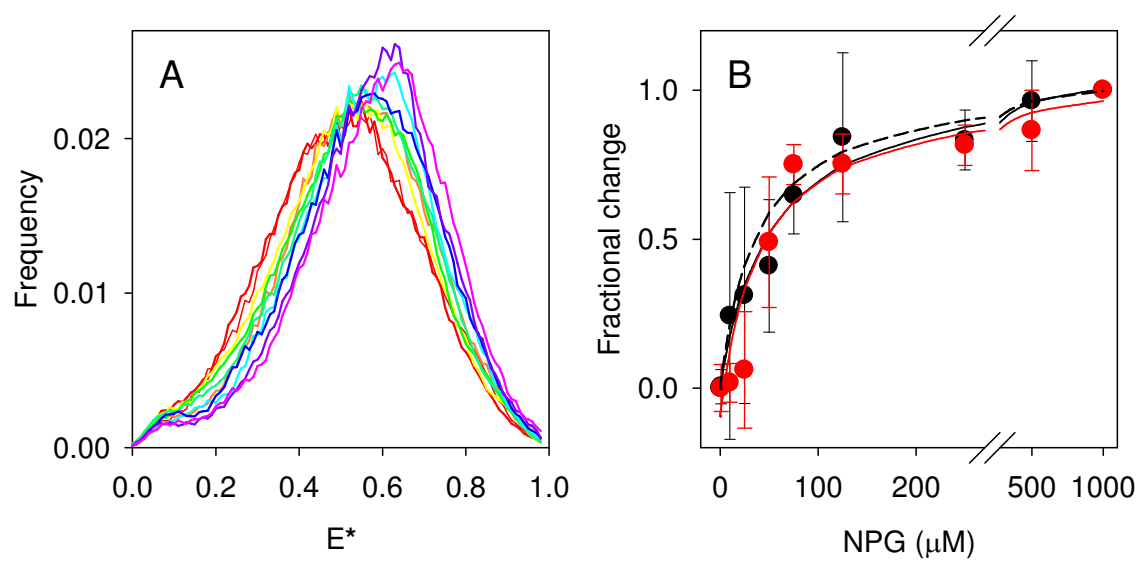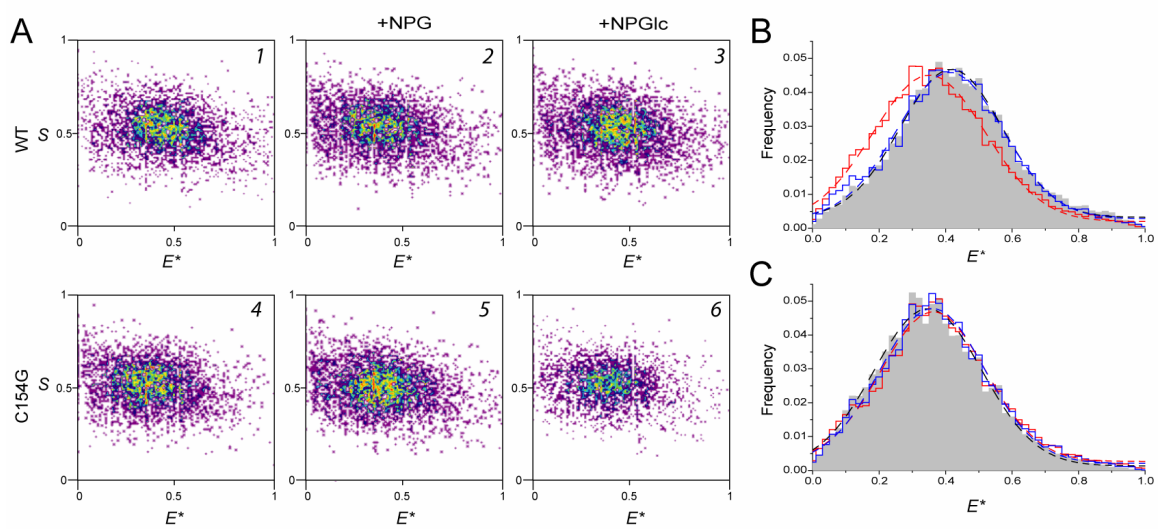**Figure 2**   **Majumdar et al.**

A

B

Figure 3 **Majumdar et al.**

Figure 4   Majumdar et al.

Figure 5 **Majumdar et al.**